

Numerical and experimental assessment of a linear aerospike

Emanuele Resta^{1,a,*}, Gaetano Maria Di Cicca^{1,b}, Michele Ferlauto^{1,c} and Roberto Marsilio^{1,d}

¹DIMEAS, Politecnico di Torino, Corso Duca degli Abruzzi 24, Turin, Italy

^aemanuele.resta@polito.it, ^bgaetano.dicicca@polito.it, ^cmichele.ferlauto@polito.it,

^droberto.marsilio@polito.it

Keywords: Aerospike, Nozzle, Experimental, Numerical

Abstract. In the present work a linear aerospike nozzle model has been studied with cold flow experiments in various working conditions. A series of numerical 3D RANS simulations have been performed in order to directly compare numerical and experimental results. Mean pressure distributions have been measured on the nozzle model symmetry plane, in order to characterize the flow evolution along the walls of the plug. The presented results show a good agreement between numerical and experimental results.

Introduction

Key requirements of future space transportation systems are a drastic reduction of launch costs and an increased reliability. Single-Stage-to-Orbit (SSTO) and Two-Stage-to-Orbit (TSTO) configurations are being studied as possible architectures of future launchers. However, the performance of the rocket engines heavily influences the possibility of realization of these vehicles. The performances of existing rocket engines are always lower than the theoretical values because of the presence of several loss mechanisms. Some examples are: the imperfect mixing of oxidizer and fuel in the combustion chamber, losses due to the process of combustion, losses for divergence and non-uniformity of the exiting flow and a non-ideal expansion of the propellants [1]. The latter source of losses is the most important. In fact, as was for the Space Shuttle Main Engine (SSME), the non-adaptation of the exhaust gases can cause up to 15% decrease in performance during certain phases of the mission [2].

A possible solution for the design of the engine of SSTO vehicles may be found in aerospike nozzles (also called plug nozzles), which represent a valid alternative to conventional bell nozzles. In fact, aerospike nozzles provide, at least theoretically, continuous altitude adaptation up to their geometrical area ratio. For high area ratio nozzles with relatively short length, plug nozzles perform better than conventional bell nozzles [2,3]. For these reasons, experimental, analytical and numerical research on plug nozzles have been performed since the 50s worldwide. One notable example of an aerospike engine project and prototype is the linear aerospike engine XRS-2200, which was selected as candidate propulsion system for the Venture Star/X33 SSTO spaceplane in the 1990s. Moreover, the use of linear aerospike nozzles has also started to spark interest regarding the propulsion of high-speed aircraft [4]. Nozzle flow control, including thrust vectoring and external flow interactions, has become increasingly relevant for the controllability of aircrafts. Fluidic thrust vectoring techniques in particular, are gaining significant interest for their advantages over traditional methods, both for use with conventional and unconventional nozzles [5,6]. One example is, for instance, differential throttling, a simple control strategy which can be applied in clustered aerospike engines with multiple independent combustion chambers. Since the mass flow rate and the pressure can be controlled independently, it is possible to generate an asymmetry in thrust, creating a lateral force component [7]. Another possible solution could be the Shock Vector Control approach, which consists in injecting a secondary flow from the plug wall. This causes the flow to separate, generating a recirculation zone on the wall and a shock wave that

deflects the incoming flow. As a result, the pressure distribution on the nozzle walls becomes asymmetric, generating a lateral thrust component [8].

The aim of the study is to compare the pressure measurements obtained with an experimental setup, which was previously designed at Politecnico di Torino [9,10], with numerical simulation results. This experimental system will be able to be fitted with different types of nozzle geometries. The mean pressure is measured along the nozzle walls on the symmetry plane, and is compared with 3D numerical results for analogous working conditions.

Test Rig Set-Up and Instrumentation

The test-rig is composed of two subsystems: the air-supply control system and the nozzle model. The first subsystem provides the prescribed inlet flow conditions and is able to manage interchangeable nozzle models, both axisymmetric and linear, for example bell/dual-bell nozzles, and aerospikes. An interfacing duct may be required to generate the correct inlet flow conditions in the axisymmetric or 2D/3D case. The test rig is positioned on a frame, as shown in Figure 1. A corrugated metal hose with an inner diameter of 25 mm is used to provide compressed air to the system. It is connected to a diffuser, followed by a flow straightener.

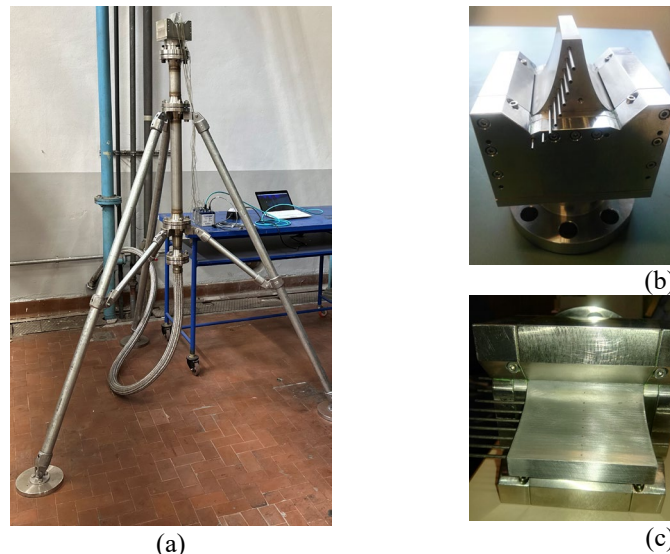


Fig. 1: Assembled Test-Rig (a). Two close-up views of the plug nozzle model (b-c)

For this work, a linear plug nozzle model was used, with a width to height throat ratio b/h_t equal to 30.41. The model is connected to the flange at the exit of the downstream duct. The exit Mach number M_e is equal to 1 and the design Nozzle Pressure Ratio NPR_d is equal to 200. Additional details on the dimensions of the nozzle plug are available in a previous paper [9].

The splines describing the plug surfaces of the nozzle have been designed using the method proposed by Angelino [11], with a tilt angle ϑ equal to 68.1° at the throat. The aerospike plug geometry is truncated at 40% of the ideal length.

Mean pressure distributions are measured along the nozzle plug using a Scanivalve[®] DSA5000 pressure scanner. This device is capable of taking up to 16 individual pressure measurements at different locations along the plug, with the use of 16 temperature compensated piezo-resistive pressure transducers. Moreover, individual 24-bit A/D converters are included for each pressure sensor. This feature allows fully synchronous data collection and data stream up to 5000Hz (samples/channel/second). One resistance temperature detector (RTD) per pressure sensor is integrated in the unit and each RTD utilizes its own 24-bit A/D converter. The system accuracy is $\pm 0.04\%$ FS for a pressure range from 0 up to 250 psi (from 0 up to 17.2 bar).

The static wall pressures are measured thanks to the orifices (with a diameter equal to 0.6 mm) drilled perpendicularly into the nozzle plug wall (see Figure 1-a). The distance between two adjacent pressure ports is equal to 7 mm. These ports are connected through small steel tubes and Teflon tubes to the Scanivalve® pressure scanner.

Numerical and Experimental Results

Numerical simulations have been performed for the same values of Nozzle Pressure Ratio (NPR) used in the experiments. The commercial solver Star-CCM+ has been utilized to perform the steady RANS simulations. The numerical scheme is second order accurate in space and first order accurate in pseudo-time. A grid of about 1.2 million cells has been utilized for these simulations.

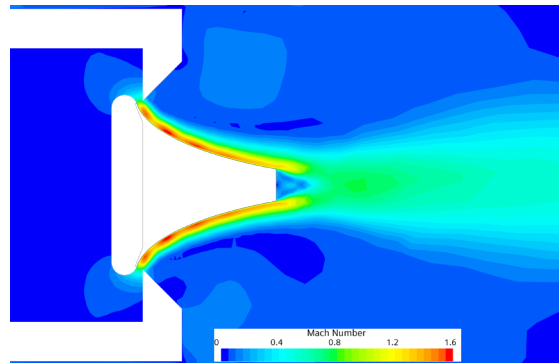


Fig. 2: Mach contour result of the flowfield in the symmetry plane of the nozzle

The Mach contour results from the numerical simulations are shown for the symmetry plane in Figure 2. The structure of the expanding flow is consistent with results from the literature regarding overexpanded flows in aerospike nozzles [2]. The presence of regions of compression and expansion can be clearly seen in this figure. A zone of recirculation on the base of the plug is also visible. In this region pressure is higher than on the walls or in the plume and that gives a positive contribution to thrust. Figure 3 shows a comparison in terms of wall static pressure between the measurements in the present experiment runs and the numerical results from the simulations. The measurements were performed for different NPRs, with the nozzle working in over-expanded conditions. The waviness of the pressure distributions highlights the presence of compression and expansion waves in the region close to the plug surface. The pressure distribution for NPR equal to 3 and 3.7 perfectly match the experimental data. What's more, there are some small differences between the numerical and experimental data for the remaining values of NPR. This could be due to numerical error of the simulation or imperfections in the manufacturing of the physical nozzle model. However, the results still match remarkably.

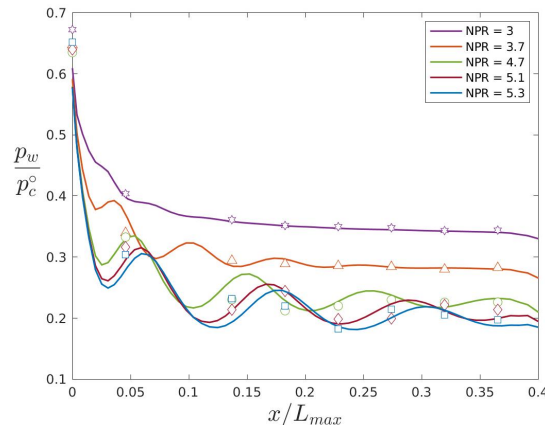


Fig. 3: Comparison between experimental and numerical wall mean pressure distributions.

Conclusions

An aerospike nozzle model has been tested experimentally to characterize the flow evolution along the walls of the plug. The experiments have been carried out in cold flow conditions at different values of NPR. The experimental results have been compared with 3D numerical simulation results, and are presented in terms of wall mean pressure distributions, and a very good agreement has been found.

References

- [1] D. Manski, G. Hagemann, “Influence of rocket design parameters on engine nozzle efficiencies”, AIAA 30th Joint Prop. Conference, 1994. <https://doi.org/10.2514/6.1994-2756>
- [2] G. Hagemann, H. Immich, T. V. Nguyen, and G. E. Dumnov, “Advanced rocket nozzles,” *Journal of Propulsion and Power*, vol. 14, no. 5, pp. 620–634, 1998. <https://doi.org/10.2514/2.5354>
- [3] R. C. Parsley, K. J. van Stelle, “Altitude Compensating Nozzle Evaluation”, AIAA Paper 92-3456, Jul. 1992. <https://doi.org/10.2514/6.1992-3456>
- [4] T. Tomita, H. Tamura, and M. Takahashi, “An experimental evaluation of plug nozzle flow field,” in 32nd AIAA Joint Prop. Conference, 1996. <https://doi.org/10.2514/6.1996-2632>
- [5] M. Ferlauto, R. Marsilio “Influence of the External Flow Conditions to the Jet-Vectoring Performances of a SVC Nozzle”, AIAA Joint Prop. Conference, Indianapolis, IN, 2019. <https://doi.org/10.2514/6.2019-4343>
- [6] S. Eilers, M. Wilson, S. Whitmore, and Z. Peterson, “Side-force amplification on aerodynamically thrust-vectoring aerospike nozzle,” *Journal of Propulsion and Power*, 2012. <https://doi.org/10.2514/6.2011-5531>
- [7] M. Ferlauto, A. Ferrero, M. Marsicovetere, and R. Marsilio, “A comparison of different technologies for thrust vectoring in a linear aerospike”, ECCOMAS WCCM 2020, Paris, 2021. <https://doi.org/10.23967/wccm-eccomas.2020.006>
- [8] E. Resta, R. Marsilio, M. Ferlauto “Thrust Vectoring of a Fixed Axisymmetric Supersonic Nozzle Using the Shock-Vector Control Method”, *Fluids*. 6(12):441, 2021. <https://doi.org/10.3390/fluids6120441>
- [9] V. Bonnet, F. Ortone, G. M. Di Cicca, R. Marsilio, and M. Ferlauto, “Cold gas measurement system for linear aerospike nozzles,” *IEEE Metrology for Aerospace 2022*, Pisa, Italy, 2022. <https://doi.org/10.1109/MetroAeroSpace54187.2022.9855979>
- [10] G. M. Di Cicca, J. Hassan, E. Resta, R. Marsilio, M. Ferlauto, “Experimental Characterization of a Linear Aerospike Nozzle Flow”, *IEEE Metrology for Aerospace 2023*, Milan, Italy, 2023. <https://doi.org/10.1109/MetroAeroSpace57412.2023.10189981>
- [11] G. Angelino, “Approximate method for plug nozzle design”, *AIAA Journal*, vol. 2, no. 10, pp. 1834–1835, 1964. <https://doi.org/10.2514/3.2682>